- Sensitivity
- W-term
- Measurement equation

Astronomical Techniques II : Lecture 13

Ruta Kale

Low Frequency Radio Astronomy (Chp. 14)
http://www.ncra.tifr.res.in/ncra/gmrt/gmrt-users/low-frequency-radio-astronomy

Synthesis imaging in radio astronomy II, Chp 19, 31, 32

Other references are given on the slides.

Sensitivity

For a single antenna:

$$\sigma_s = \frac{2kT_{\mathrm{sys}}}{A_{\mathrm{eff}}(\Delta\nu_{\mathrm{RF}}\tau)^{1/2}}$$

For an interferometer:

$$\sigma_s = \frac{2^{1/2}kT_{\mathrm{sys}}}{A_{\mathrm{eff}}(\Delta\nu_{\mathrm{RF}}\tau)^{1/2}}$$

The sensitivity of an interferometer is square root 2 times better than that of each antenna but the same factor worse than a single antenna with an area of two antennas.

For an interferometer with N elements:

$$\sigma_s = \frac{2kT_{\rm sys}}{A_{\rm eff}[N(N-1)\Delta\nu_{\rm RF}\tau]^{1/2}}$$

In the limit of large N, N(N-1) → N^2 and the point source sensitivity of an interferometer approaches that of a single antenna whose area equals the total effective area NA_{eff} of the interferometer.

In practice interferometers are slightly less sensitive due to the effects of sampling and digitizing.

Sensitivity of an image

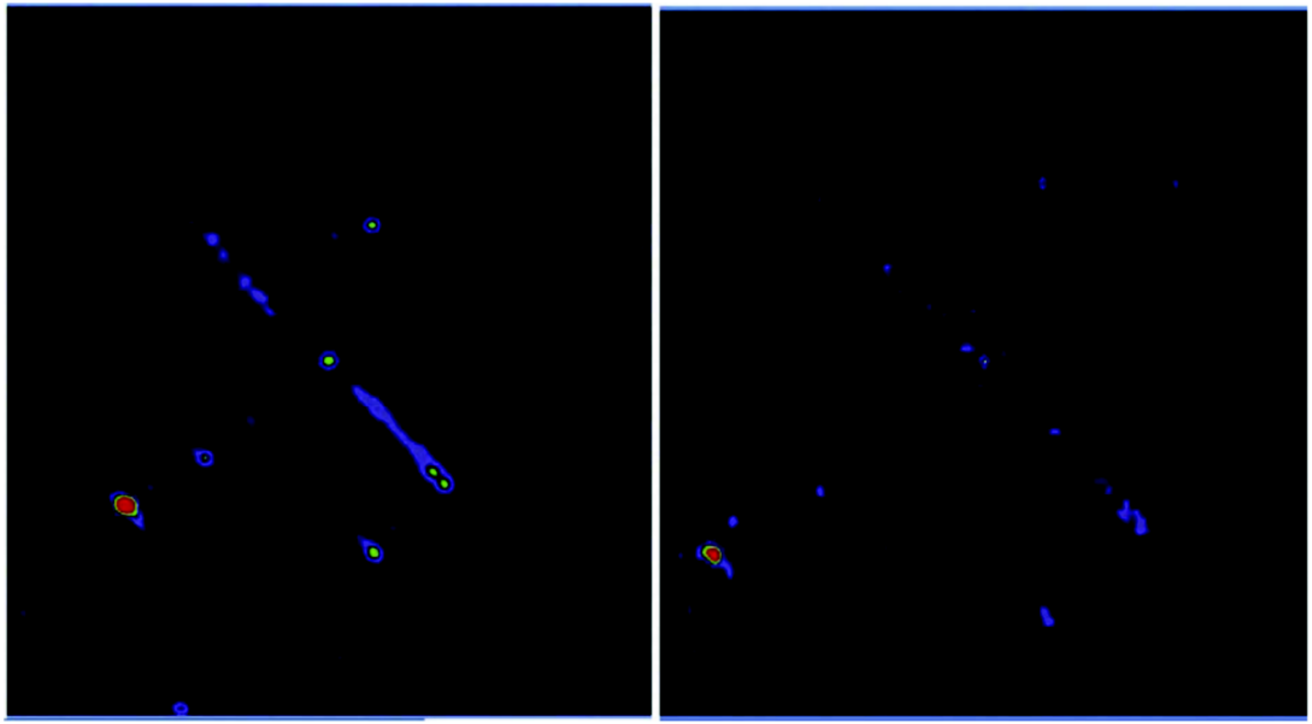

Dynamic range and fidelity

Dynamic range: Peak in the image/ image noise
Usually used for point source sensitivity.

For images of extended sources, image fidelity is also important.

Image fidelity is affected by gaps in uv-coverage, errors in deconvolution and self-calibration.

Dynamic range is primarily a diagnostic of instrumental performance and calibration. Also used to quantify fidelity as improving DR does finally lead to better image fidelity. Depending on the science goal the images are made with different weights and self-calibration strategy and image noise is not the only indicator of image quality.

SIRA II, Chp 13; Example from P. Chandra

GMRT sensitivity

$$\mathrm{RMS} = \frac{T_{\mathrm{sys}}}{G\sqrt{[N(N-1)/2] \times N_{pol} \times 2 \times \Delta\nu \times \Delta t}} \quad \text{Jy}$$

Tsys:

150 MHz: 615 K†
235 MHz: 237 K†
325 MHz: 106 K
610 MHz: 102 K
1280 MHz: 73 K

Antenna gain:

150 MHz: 0.33 K Jy^{-1} Antenna^{-1}
235 MHz: 0.33 K Jy^{-1} Antenna^{-1}
325 MHz: 0.32 K Jy^{-1} Antenna^{-1}
610 MHz: 0.32 K Jy^{-1} Antenna^{-1}
1280 MHz: 0.22 K Jy^{-1} Antenna^{-1}

For preparing observations, Exposure Time Calculator (ETC)

http://www.ncra.tifr.res.in:8081/~secr-ops/etc/rms/rms.html

Confusion noise

Classical confusion (Condon 1974)

- When the density of faint extragalactic sources becomes too high for them to be clearly resolved by the array, the deflections in the image will include the sum of all the unresolved sources in the main lobe of the synthesised beam. This effect is known as classical confusion.
- It only depends on the source counts and the synthesised beam area.

Sidelobe confusion

- Noise is introduced into an image from the combined sidelobes of undeconvolved sources, i.e. from the array response to sources below the source subtraction cut-off limit and to sources outside the imaged FoV.

Confusion noise

Confusion "noise" is given by,

$$\sigma_c = \rho \sqrt{\int B^2(\Omega)\, d\Omega \int S^2 n(S)\, dS}$$

B is a primary beam response, n(S) is the source distribution function (the number of sources with flux densities between S and S+dS) and ρ is the r.m.s. fluctuation of the synthesized beam.

Confusion noise can be expressed as a weighted, incoherent sum of the sidelobe responses to all sources in the primary beam.

At low frequencies, confusion noise can be given as (Condon 2012)

$$\sigma_c^* = 1.2\mu\mathrm{JyBeam}^{-1} \left[\frac{\nu}{3\ \mathrm{GHz}}\right]^{-0.7} \left[\frac{\theta}{8''}\right]^{10/3}$$

Not a problem until the rms is higher than confusion noise; otherwise it is referred to as confusion limited array – only way is to increase the baseline length.

Perley and Erickson 1984; Condon 2012; Patra et al 2019

Visibilities: the w-term

$$V(u,v,w) = \int_{-\infty}^{\infty}\int_{-\infty}^{\infty} I(l,m) e^{-2\pi i\left[ul+vm+w\left(\sqrt{1-l^2-m^2}-1\right)\right]} \frac{dl\,dm}{\sqrt{1-l^2-m^2}}$$

The w-term:

$$w\sqrt{1-l^2-m^2}$$

The origin of the w-term is purely geometrical and arises due to the fact that fringe rotation effectively phases the array for a point in the sky called the phase center.

Visibilities: when can we ignore the w-term?

$$V(u,v,w) = \int_{-\infty}^{\infty}\int_{-\infty}^{\infty} I(l,m) e^{-2\pi i\left[ul+vm+w\left(\sqrt{1-l^2-m^2}-1\right)\right]} \frac{dl\,dm}{\sqrt{1-l^2-m^2}}$$

All the visibilities lie in a plane. In this case

$$w = \alpha u + \beta v$$

Condition met when:
a) 1 dim E-W array
b) 2 dim array short observations
c) if the 2 dim array located at the pole
d) narrow field of view

$$V(u,v) \sim \int\int I(\ell,m)\, e^{-2\pi i[u\ell+vm]} d\ell\, dm$$

Non-coplanar baselines

The phase error incurred by ignoring the w-term can be given as (in radians):

$$\text{error} \approx \pi w \theta^2 \qquad \theta \equiv \sqrt{l^2 + m^2}$$

Linear with w

Quadratic with distance
from the phase center

$$V(u,v,w) = \int_{-\infty}^{\infty} \int_{-\infty}^{\infty} I(l,m) e^{-2\pi i \left[ul + vm + w\left(\sqrt{1-l^2-m^2}-1\right)\right]} \frac{dl\, dm}{\sqrt{1-l^2-m^2}}$$

For large fields of view this term is going to affect the image.

Example

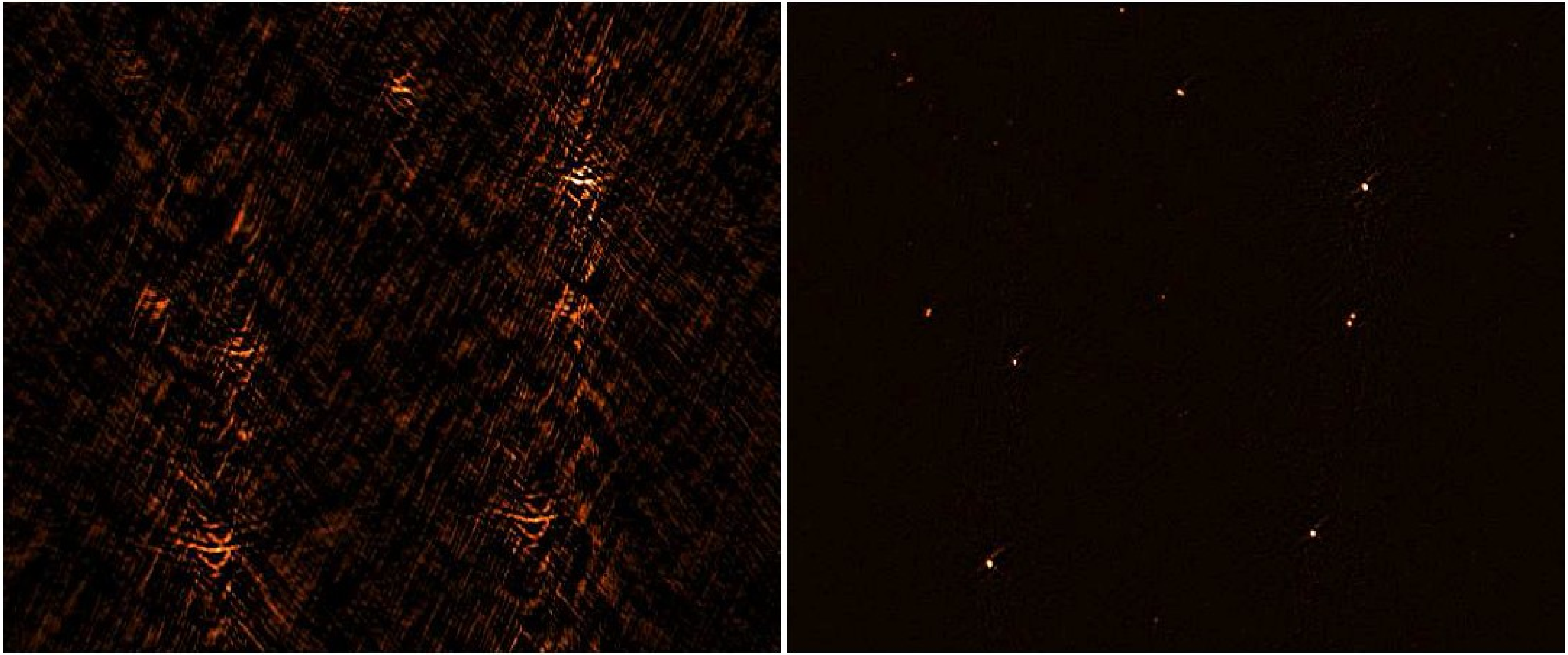

GMRT 235 MHz image: Portion of the image that is about 0.8 degrees from the phase tracking centre.

Example

Example: A source located 47.5’ away from phase center imaged using full uv-coverage in VLA-B array ignoring the w-term.

In the right panel the same source when only a short time interval of 30 min was imaged is shown.

Distortion and error in position are the effects of ignoring the w-term.

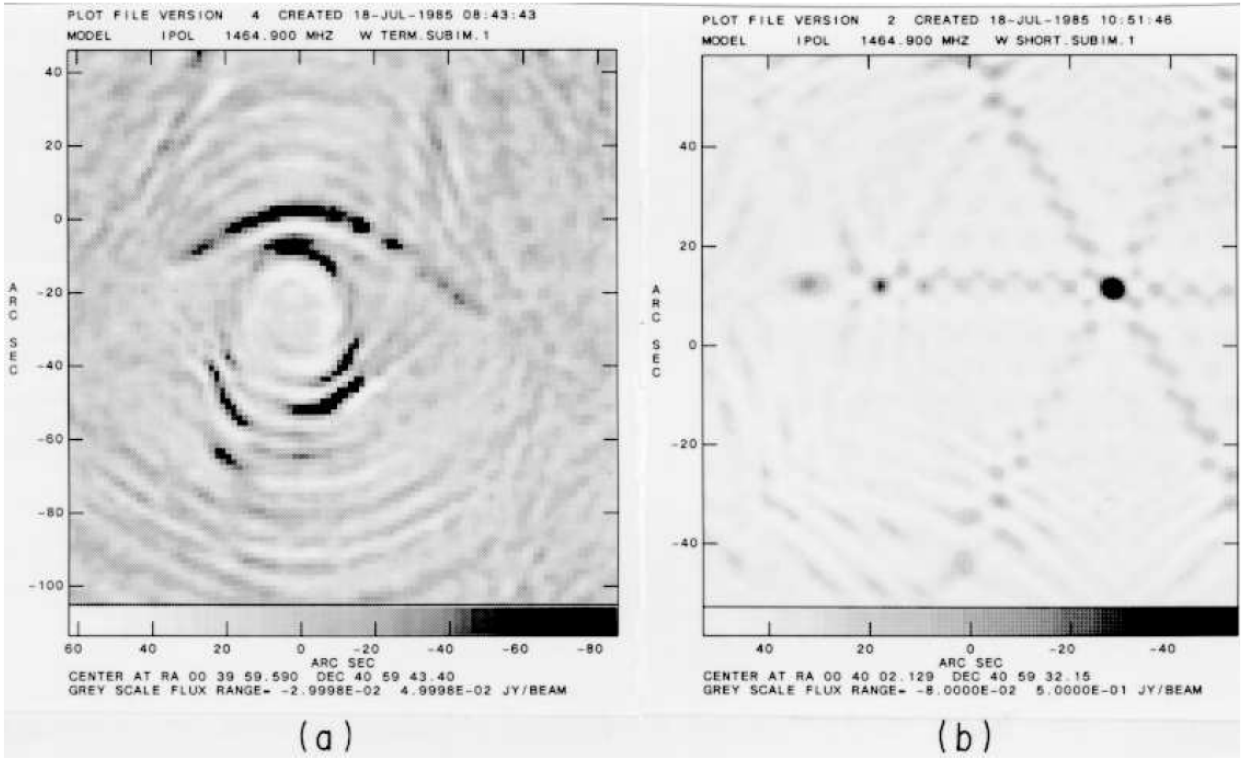

Figure 17–5. **(a)** The response of the VLA to a point model source 47′.5 in RA from the phase center, for full coverage in the VLA **B** configuration at 1.4 GHz. Zeros on the axes label the correct position of the source; the model contained 1 Jy, but the peak in the image is 0.071 Jy. **(b)** Similar to (a), but made using the (u, v) coverage corresponding to only 30 minutes of observation. The peak in the image is 0.948 Jy.

Non-coplanar baselines

The position error on ignoring w-term:

$$\text{position error} \approx \frac{\theta^2}{2 \times 2.06 \times 10^5} \sin z$$

z is the zenith angle

If this is smaller than the synthesized beam it can be ignored.

Example: A source located 47.5' away from phase center Imaged using full uv-coverage in VLA-B array ignoring The w-term.
In the right panel the same source when only a short time Interval of 30 min was imaged is shown.
Distortion and error in position are the effects of ignoring the w-term.

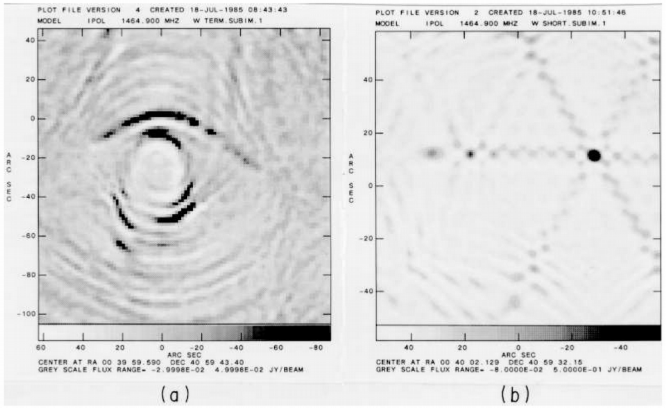

Image volume

$$V(u,v,w) = \int_{-\infty}^{\infty}\int_{-\infty}^{\infty} I(l,m) e^{-2\pi i\left[ul+vm+w\left(\sqrt{1-l^2-m^2}-1\right)\right]} \frac{dl\,dm}{\sqrt{1-l^2-m^2}}$$

Multiply through with $e^{-2\pi i w}$

$$V'(u,v,w) = \iint I(l,m) e^{-2\pi i\left[ul+vm+w\sqrt{1-l^2-m^2}\right]} \frac{dl\,dm}{\sqrt{1-l^2-m^2}}$$

$$n = \sqrt{1-l^2-m^2}$$

$$F(l,m,n) = \iiint V'(u,v,w) e^{2\pi i(ul+vm+wn)}\, du\, dv\, dw$$

3D FT relation ?

Image volume

$$F(l,m,n) = \iiint V'(u,v,w) e^{2\pi i(ul+vm+wn)}\, du\, dv\, dw$$

$$F(l,m,n) \;=\; \iiint \left\{ \iint \frac{I(l',m')}{\sqrt{1-l'^2-m'^2}} e^{-2\pi i(ul'+vm'+w\sqrt{1-l'^2-m'^2})}\, dl'\, dm' \right\} e^{2\pi i(ul+vm+wn)}\, du\, dv\, dw$$

$$F(l,m,n) = \iint \left\{ \iiint \frac{I(l',m')}{\sqrt{1-l'^2-m'^2}} e^{-2\pi iu(l'-l)} e^{-2\pi iv(m'-m)} e^{-2\pi iw(\sqrt{1-l'^2-m'^2}-n)}\, du\, dv\, dw \right\} dl'\, dm'$$

Integrals over u, v and w to be evaluated

The integrals over u, v and w can be evaluated using:

$$\delta(l'-l) = \int e^{-2\pi i u(l'-l)}\, du$$

In the equation:

$$F(l,m,n) = \iint \left\{ \iiint \frac{I(l',m')}{\sqrt{1-l'^2-m'^2}} e^{-2\pi i u(l'-l)} e^{-2\pi i v(m'-m)} e^{-2\pi i w(\sqrt{1-l'^2-m'^2}-n)}\, du\, dv\, dw \right\} dl'\, dm'$$

$$F(l,m,n) = \iint \frac{I(l',m')}{\sqrt{1-l'^2-m'^2}} \delta(l'-l)\delta(m'-m)\delta(\sqrt{1-l'^2-m'^2}-n)\, dl'\, dm'$$

$$F(l,m,n) = \frac{I(l,m)\delta(\sqrt{1-l^2-m^2}-n)}{\sqrt{1-l^2-m^2}}$$

“Image volume”: but as such the emission is confined to a surface of a sphere of radius n.

3D FFT

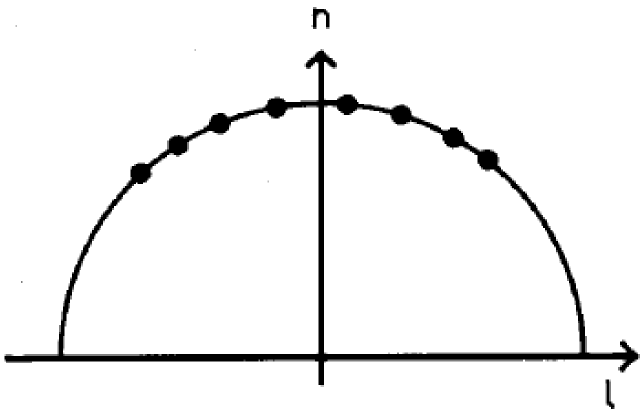

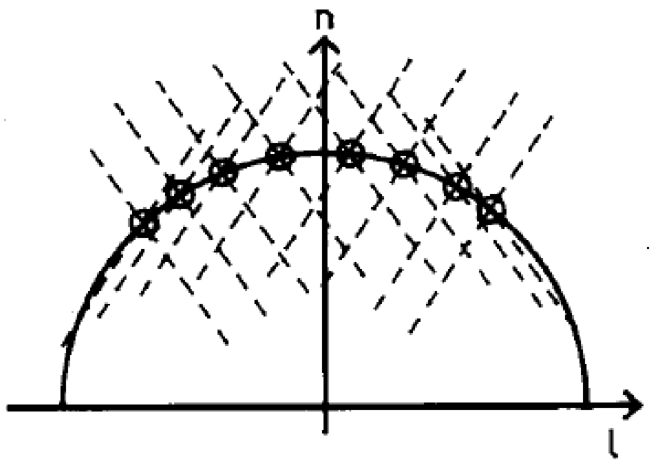

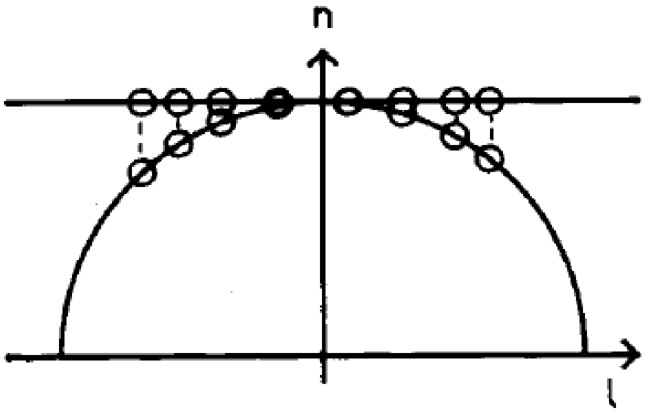

Slice through m=0

Shows the distribution on the sphere.

Convolution with dirty beam results in sidelobes.

After deconvolution sources restored to a projected plane.

W-term: geometric

Two interferometers: one on a plane and another on a slope- has a large w-component.
The phase of arriving signal at an angle w.r.t that of a signal at the phase tracking center.

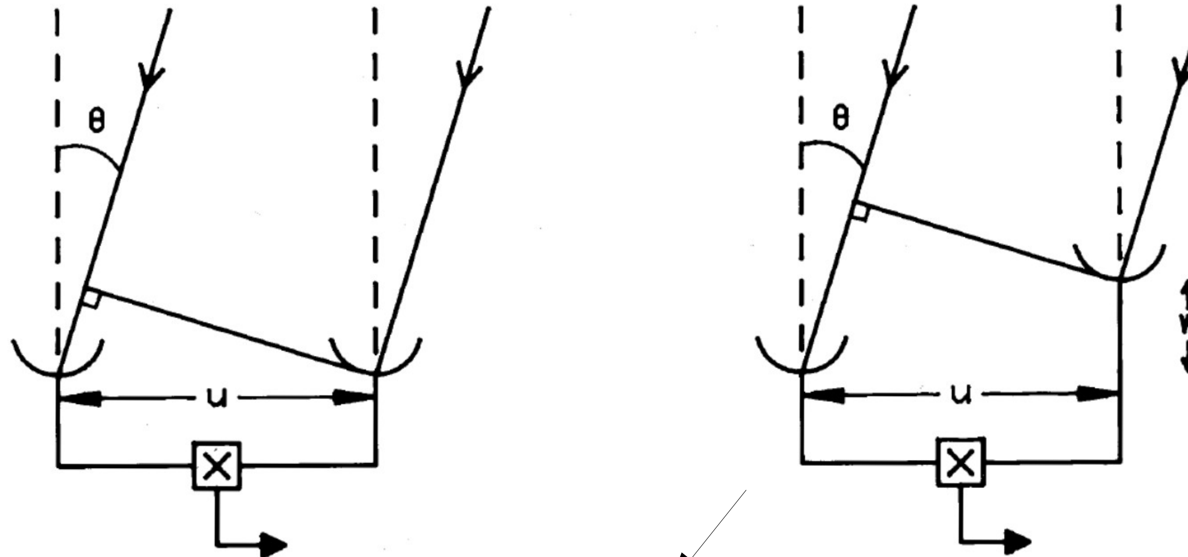

$$\phi_{\text{ref}} = 0$$

$$\phi_{\text{level}} = 2\pi u l$$

u is the baseline and l is, $l = \sin\theta$

$$\phi_{\text{ref}} = 2\pi w$$

$$\phi = 2\pi(w + u\tan\theta)\cos\theta$$

Relative phase is $2\pi[w(\cos\theta - 1) + u\sin\theta]$

$$\phi_{\text{tilt}} = 2\pi\left[ul + w\left(\sqrt{1-l^2} - 1\right)\right]$$

Bandwidth broadening in 3D

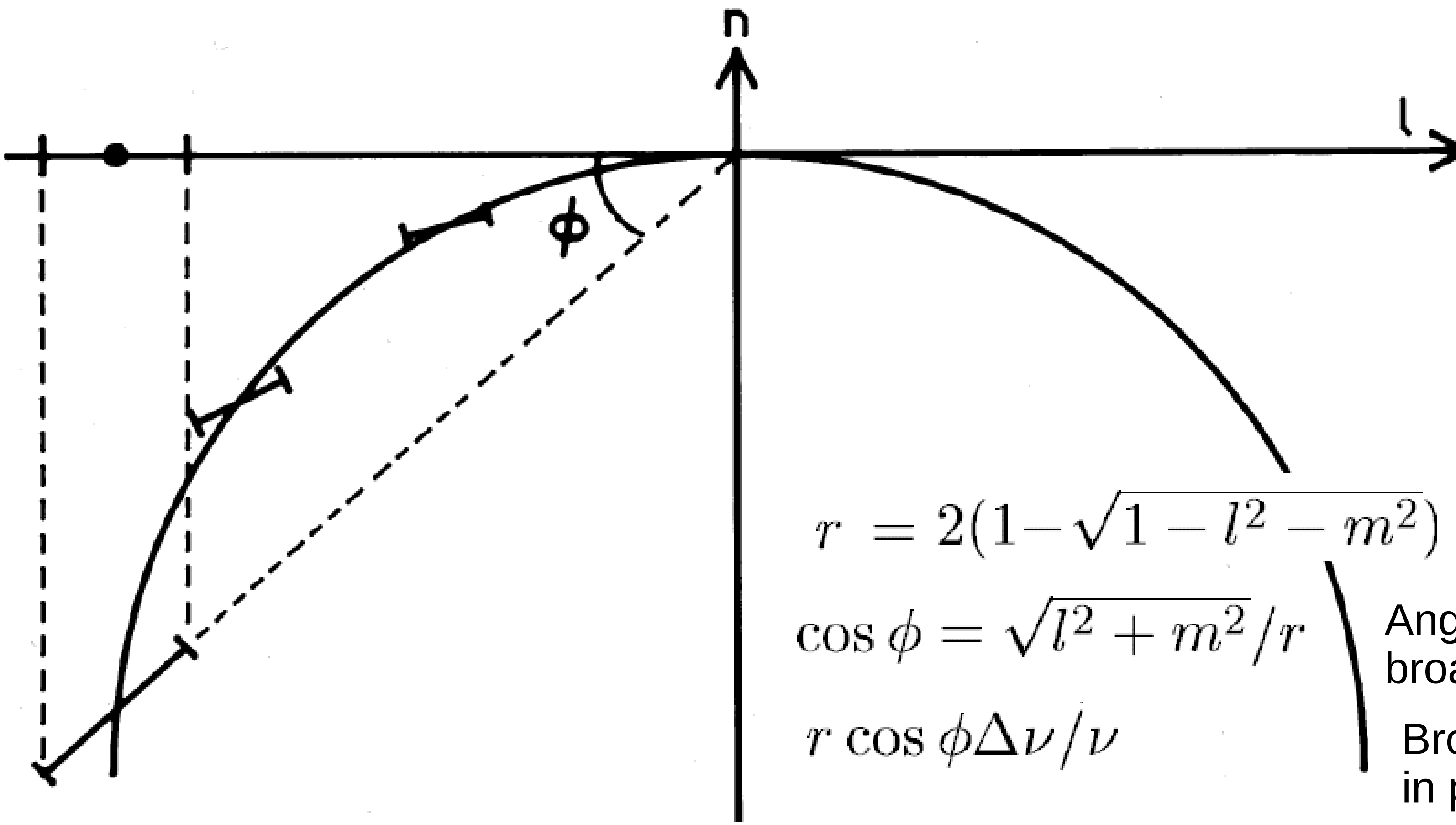

$$r = 2(1 - \sqrt{1 - l^2 - m^2})$$

$$\cos\phi = \sqrt{l^2 + m^2}/r$$

Angle of broadening

$$r \cos\phi \Delta\nu/\nu$$

Broadening in projection

$$\sqrt{l^2 + m^2}\,(\Delta\nu/\nu)$$

Depends on radial distance and fractional bandwidth

3D FFT

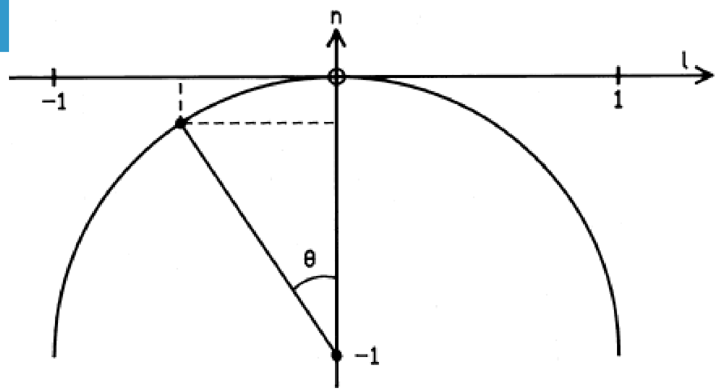

Needs good sampling in n-axis otherwise severe aliasing.

How many n-planes are required ?

$$\theta \approx \lambda / B_{\max}$$

$$\delta n \approx \lambda / 2B_{\max}$$

$$n_d = 1 - \cos\theta \approx \theta^2/2$$

$$N_{\text{planes}} = n_d/\delta n = B\theta^2/\lambda$$

$$N_{\text{planes}} = \lambda B/D^2$$

Table 19–1
Number of n-axis Planes Required for 3–D Imaging

	— VLA Configuration —			
Wavelength	**A**	**B**	**C**	**D**
4 m	225	68	23	7
1 m	56	17	6	2
20 cm	11	4	2	1
6 cm	4	2	1	1

The number of planes on n-axis equals the FoV in radians times the FoV in synthesized beamwidths.

Polyhedron imaging

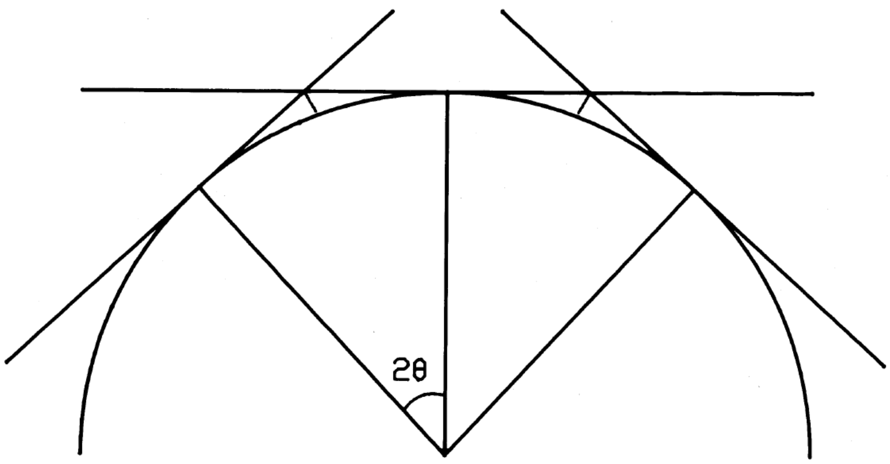

Approximate sphere with multiple tangent planes where 2D approx. valid.

Separation between the tangent plane and image sphere is:

$$1 - \cos\theta \approx \theta^2/2$$

Theta is the angle from phase tracking center.

The maximum undistorted field of view in a 2D image:

$$\theta_{\rm max} = \sqrt{\lambda/B} \approx \sqrt{\theta_{\rm syn}}$$

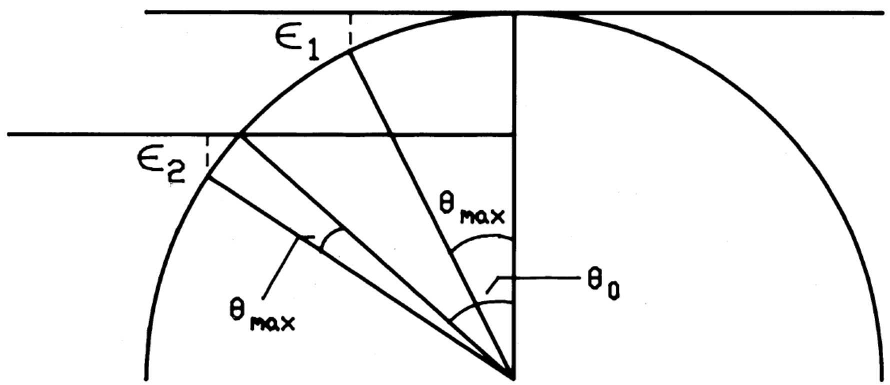

By simply phase shifting the image plane and not rotating the baselines:

$$\epsilon_2 = \cos(\theta_0) - \cos(\theta_0 + \theta) \approx \theta\theta_0$$

$$\theta_{\rm max} = \lambda/(2B\theta_0)$$

$$\theta_0 \approx \lambda/D$$

$$\theta_{\rm max} \approx D/2B$$

For VLA A-array this is 70”

Not rotating the baselines leads to very small undistorted FoV

Polyhedron imaging

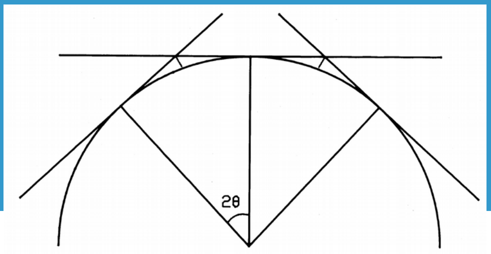

The maximum separation between the tangent plane and the sphere should be less than

$$f\lambda/2B$$

The actual separation between a plane and a sphere is

$$1 - \cos\theta$$

Using small angle approximation we get:

$$\theta^2 < f\lambda/2B$$

The number of images required to fill the primary beam is the radio of the primary beam solid angle to the sub-field solid angle:

$$N_{\mathrm{poly}} = 2B\lambda/fD^2$$

For critical sampling f=1.

Polyhedron imaging is commonly used for VLA and GMRT – implemented in AIPS and CASA.

W-projection

Cornwell et al 2008

Implemented in CASA

When the term $2\pi w(\sqrt{1-\ell^2-m^2}-1)$ is comparable to or exceeds unity, the two dimensional FT does not work.

The value of the extra phase term assuming maximum w ~ B/λ is roughly:

$$\frac{B\lambda}{D^2} = \left(\frac{r_F}{D}\right)^2$$

Here r_F is the Fresnel zone diameter for a distance B.

$N_F = \frac{D^2}{B\lambda}$ < 1 when effects due to non-co-planar baselines start affecting.

Small apertures, long baselines or long wavelengths.

W-projection basis

Frater and Docherty 1980 noted that projection from a single plane w to w=0 is possible.

In w-projection the fact that it is possible to project any (u,v,w) to w = 0 is used by choosing appropriate convolution function.

$$V(u,v,w) = \int \frac{I(\ell,m)}{\sqrt{1-\ell^2-m^2}} e^{-2\pi i[u\ell+vm+w(\sqrt{1-\ell^2-m^2}-1)]} d\ell dm$$

$$G(\ell,m,w) = e^{-2\pi i[w(\sqrt{1-\ell^2-m^2}-1)]}$$

$$V(u,v,w) = \int \frac{I(\ell,m)}{\sqrt{1-\ell^2-m^2}} G(\ell,m,w)\; e^{-2\pi i[u\ell+vm]} d\ell dm$$

$\tilde{G}(u,v,w)$

Is the FT of G(l,m,w)

$$V(u,v,w) = \tilde{G}(u,v,w) * V(u,v,w=0)$$

W-projection

$$G(\ell, m, w) = e^{-2\pi i[w(\sqrt{1-\ell^2-m^2}-1)]}$$

Small angle approximation.

$$G(\ell, m, w) = e^{\pi i[w(l^2+m^2)]}$$

FT

$$\tilde{G}(u, v, w) = \frac{i}{w} e^{-\pi i[\frac{(u^2+v^2)}{w}]}$$

The visibility for any non-zero w can be calculated from the visibility for w=0 by convolution with the known function G.

The origin of this is the fact that the brightness is confined to a 2-dimensional plane.

W-projection

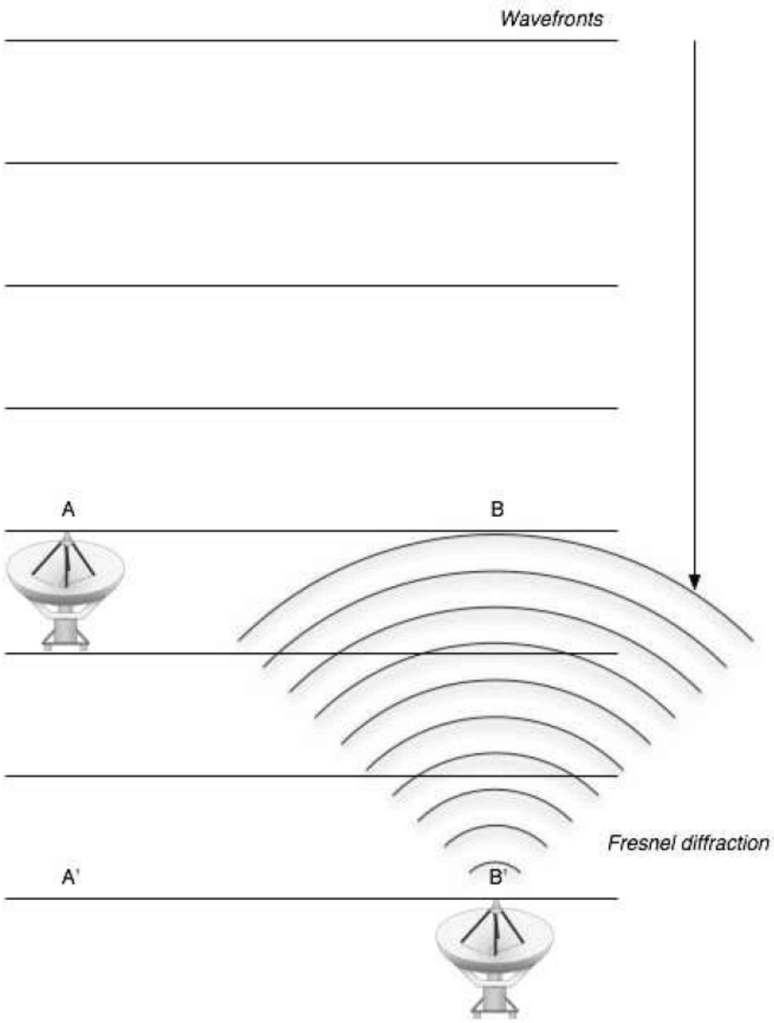

We want to correlate wavefronts at A and B but what we have is A and B'.
On propagating from B to B' the wavefront diffracts which results in the fact that AB and AB' are different.

The resulting convolution relationship is due to Fresnel diffraction of the electric field during propagation from B to B'.
The size of diffraction pattern is

$$r_F / \lambda \sim \sqrt{w}$$

An interferometer with the same (u,v) but non-zero w does not measure a "single" Fourier component but one can recover information within r_F / λ

W-stacking

Humphreys and Cornwell 2011
Offringa et al 2014

W-stacking is an alternative implementation of w-projection.

In w-projection the uv-samples are convolved with a w-proj kernel before FFT.

In w-stacking instead the correction is done as a multiplication after the FFT.

$$\frac{I'(l,m)}{\sqrt{1-l^2-m^2}} = e^{2\pi i w(\sqrt{1-l^2-m^2}-1)} \iint V(u,v,w) \times \; e^{2\pi i(ul+vm)} du dv$$

$$\frac{I'(l,m)\,(w_{\max}-w_{\min})}{\sqrt{1-l^2-m^2}} = \int_{w_{\min}}^{w_{\max}} e^{2\pi i w(\sqrt{1-l^2-m^2}-1)} \times \iint V(u,v,w) e^{2\pi i(ul+vm)} du dv dw.$$

W-stacking

$$\frac{I'(l,m)\,(w_{\max}-w_{\min})}{\sqrt{1-l^2-m^2}} = \int\limits_{w_{\min}}^{w_{\max}} e^{2\pi i w(\sqrt{1-l^2-m^2}-1)} \times \iint V(u,v,w) e^{2\pi i(ul+vm)} du dv dw.$$

Expressing it in this form so that integration over u and v can become an inverse FFT and the integration over w becomes a summation.

The sky function can be reconstructed by:

i) gridding samples with equal w-value on a uniform grid

ii) calculating the inverse FFT

Iii) applying the direction dependent phase shift $e^{2\pi i w(\sqrt{1-l^2-m^2}-1)}$

iv) repeating this for all values of w and adding the results

v) applying the final scaling.

“WSClean”: Offringa et al 2014

Hamaker, Bregman, Sault Measurement Equation

Jones matrices:

Electric field of a mono-chromatic wave

$$E_0 \cos(\omega t + \phi) \qquad\qquad E = E_0 \exp(i\phi)$$

If E_R and E_L are the complex amplitudes of right and left circularly polarized components of a wave respectively, the output polarization states are a linear combination of the input states:

$$\begin{pmatrix} E'_{\mathrm{R}} \\ E'_{\mathrm{L}} \end{pmatrix} = \begin{pmatrix} a & b \\ c & d \end{pmatrix} \begin{pmatrix} E_{\mathrm{R}} \\ E_{\mathrm{L}} \end{pmatrix}$$

Jones matrix,
Jones 1941

$$\mathbf{J}_{\mathrm{overall}} = \mathbf{J}_1 \mathbf{J}_2 \mathbf{J}_3$$

In our context the Jones matrices are:

$$\mathbf{J}_{\text{gain}} = \begin{pmatrix} g_{\text{R}} & 0 \\ 0 & g_{\text{L}} \end{pmatrix}$$

$$\mathbf{J}_{\text{leakage}} = \begin{pmatrix} 1 & D_{\text{R}} \\ -D_{\text{L}} & 1 \end{pmatrix}$$

Jones matrix will vary from antenna to antenna and will be function of time and frequency.

Jones matrices are combined multiplicatively, even complicated systems can be handled.